Ferroelectric soft mode and relaxation behavior in a molecular-dynamics simulation of $KNbO_3$ and $KTaO_3$

M. Sepliarsky, M. G. Stachiotti, and R. L. Migoni
Instituto de Física Rosario and Facultad de Ciencias Exactas, Ingeniería y Agrimensura (UNR), 27 de Febrero 210 Bis, 2000 Rosario, Argentina
(Received 15 January 1997)

A molecular-dynamics simulation is performed for $KTaO_3$ and the paraelectric phase of $KNbO_3$ in the framework of the nonlinear oxygen polarizability model. The dynamical structure factor for wave vector $\mathbf{q}=0$ is studied as a function of temperature. In $KNbO_3$ a peak corresponding to the ferroelectric mode can hardly be identified only near the melting point. It coexists with a well developed central peak which grows in intensity and narrows with decreasing temperature. The latter is correlated with the observation of a relaxation dynamics between off-center minima of the effective potential for the soft-mode coordinate. The soft-mode peak shifts to higher frequencies and gains intensity as the temperature is further increased above the melting point, while the central peak disappears. This behavior constitutes theoretical evidence of a crossover from a displacive to an order-disorder dynamical regime near the ferroelectric phase transition in $KNbO_3$. This crossover was originally postulated to interpret the experimental data. Although these are available in the lower temperature range where the soft mode is not observed as a separate excitation, a coexistence of both dynamics had to be proposed to interpret the various experiments. In $KTaO_3$ we observe a well-defined ferroelectric-mode peak which softens with temperature in good agreement with experimental data. [S0163-1829(97)00522-5]

I. INTRODUCTION

Both $KTaO_3$ and $KNbO_3$ exhibit the cubic perovskite structure at high temperatures. While $KTaO_3$ does not undergo any phase transition and remains paraelectric down to temperatures of 0 K, $KNbO_3$ becomes ferroelectric at 708 K, with a tetragonal distortion and polarization along a [100] direction, transforms to orthorhombic with [110] polarization at 498 K, and finally settles in a rhombohedral phase with [111] polarization below 263 K. The polarization of the three ferroelectric phases is mainly related to the relative Nb-oxygen octahedron displacement.

In the framework of the nonlinear oxygen polarizability (NOP) model, we evaluated recently the energy as a function of Nb displacements on a [011] plane which contains the above directions.[1] In agreement with previous semiempirical[2] and *ab initio*[3] calculations, we obtained an energy maximum at the octahedron center, absolute minima on the [111] directions, lower saddle points on the [110] directions, and higher saddle points on the [100] directions. The relative energy values of the NOP model and local-density approximation calculations show a good quantitative agreement as well. The presence of the [111] minima has been confirmed by an extended x-ray-absorption analysis.[4] Such energy behavior is consistent with the sequence of transitions observed in $KNbO_3$, as predicted by an early proposed eight-site model.[5,6] This order-disorder model had been initially developed in order to explain the markedly anisotropic diffuse scattering observed for x rays. Further evidence of an order-disorder behavior was provided by infrared spectroscopy[7] and the direct observation of a relaxation dynamics through a central component in the Raman spectrum.[8,9] A similar order-disorder behavior has been observed in $BaTiO_3$,[5,9–12] which displays the same sequence of transitions. According to the eight-site model, all sites are visited with equal probability by the *B* ion (Nb or Ti) in the cubic phase. Four sites with equal projection along one of the cubic axes become preferentially populated in the tetragonal phase. Among these only two nearest-neighbor sites remain most probable in the orthorhombic phase, and finally only one site is occupied in the rhombohedral phase.

A ferroelectric soft mode is very well defined in $KTaO_3$, as observed by various techniques.[13–17] It softens steadily with cooling until 0 K is approached, where it remains stable just due to quantum fluctuations. A quite similar behavior has been observed in $SrTiO_3$, which induced these two compounds to be termed quantum paraelectrics. A relaxational dynamics has been observed in addition to the soft-mode dynamics in the quantum regime of both compounds.[18] Several attempts have been made to observe the ferroelectric mode also in $KNbO_3$ (Refs. 7, 19) and $BaTiO_3$;[20,21] however, the results had to be interpreted in terms of an overdamped oscillator with such a high damping that it could hardly be distinguished from a relaxator. In fact, an unified interpretation of the infrared reflectivity, dielectric, Raman, and hyper-Raman scattering data for $KNbO_3$ has been given by assuming the coexistence of a relaxational mode and a soft phonon which is extremely overdamped in the cubic and tetragonal phases.[8] The thus obtained frequency of the ferroelectric mode softens continuously throughout the cubic, tetragonal, and orthorhombic phases without vanishing at any transition. A crossover from a displacive (soft phonon) to an order-disorder (relaxation) behavior could occur at very high temperatures in the cubic phase, since the ferroelectric mode is overdamped ($\gamma_F/\omega_F > \sqrt{2}$) below at least 1200 K.[7] An analogous behavior is observed in $BaTiO_3$.[10]

Theoretically, a crossover from a soft-mode to a relaxational dynamics, with the signature of a central peak in the

 © 1997 The American Physical Society

dynamic response and precursor order clusters, has been predicted within a qualitative model with on-site double-well potential and intersite harmonic interaction;[22–24] however, a quantitative account of the overall behavior in $KNbO_3$ and $BaTiO_3$ is still missing. An accurate description of the ferroelectric soft-mode regime in ABO_3 perovskites has been given on the grounds of the NOP model.[25] This model emphasizes the large anisotropic polarization effects at the oxygens produced by variations of the O-*B* distance. Such effects are expected in view of the strong environment-dependent oxygen polarizability and its enhancement through hybridization between oxygen *p* and transition-metal *d* orbitals. Recent electronic-structure calculations[3,26–28] have demonstrated that hybridization between oxygen and transition-metal states is an important feature for driving the ferroelectric instability. Thus a shell model was proposed where the only source of lattice anharmonicity is an interaction term of fourth order in the oxygen shell-relative-to-core displacement component along the O-*B* bond. The harmonic part of the model is unstable against the ferroelectric mode displacements in the cubic structure. This happens essentially because the strong Coulomb O-*B* attraction overcomes the repulsive forces that hold the *B* ion at the cubic cell center. Therefore the stability should be provided by the fourth-order term. This has been harmonically approximated by temperature averaging a pair of displacements, which is evaluated self-consistently. Hence the temperature dependence of the complete phonon dispersion can be calculated. The effective harmonic term stabilizes the ferroelectric mode thus providing its temperature dependence. Applications to $KTaO_3$,[25,17] $SrTiO_3$,[25] $KNbO_3$,[29] $BaTiO_3$,[30] as well as the mixed compound $KTa_{1-x}Nb_xO_3$ (Ref. 29) for all Nb concentrations, lead to results in excellent agreement with the experimental phonon data.

However, the self-consistent treatment of the quartic interaction in the NOP model washes out the potential maximum at the cubic structure in terms of the soft-mode coordinate. It therefore excludes a relaxation behavior, which has wrongly led to the conclusion that the NOP model is purely displacive. In order to test the capability of the model to describe a crossover from displacive to order-disorder transition mechanism, a qualitative study with a simplified two-dimensional diatomic version of the model was performed.[31] To this purpose the instability originated by competition between short-range and Coulomb forces was simulated by taking a quartic double-well potential for the core-shell interaction at one of the atomic units, while the other was considered rigid, and only short-range interatomic forces were left. A molecular-dynamics simulation with this model allowed us to observe, in addition to the soft mode, the appearance of a central peak in the dynamical structure factor, a local relaxation dynamics, and fluctuating precursor domains on approaching the transition.

In this paper we analyze the dynamical structure factor obtained through molecular-dynamics simulations at several temperatures in the paraelectric phase of $KNbO_3$ and $KTaO_3$. The validity of any potential simulation study depends, to a considerable extent, on the quality of the pair potentials used. Taking into account our previously mentioned results,[1] we consider that our model, even in the harmonic approximation for the short-range and Coulomb interactions, is a very reliable starting point to be used for atomistic simulations of both compounds. Preliminary results presented at the 8th European Meeting on Ferroelectricity[32] did not allow the observation of a soft-mode peak in $KNbO_3$. We show here that it appears at very high temperatures. Also we have solved problems in the thermalization of the simulation which were encountered in the preliminary calculations and arise from the high degree of harmonicity of the model.

II. MODEL AND COMPUTATIONAL DETAILS

We summarize briefly the main characteristics of the NOP model, which has been described in detail elsewhere.[25,17] It is a shell model with isotropic core-shell couplings (k_A,k_B) and shell charges (Y_A,Y_B) for the *A* and *B* ions in the ABO_3 system. For the O ions two different harmonic core-shell couplings (k_{OB},k_{OA}) are considered, depending on whether the displacement of the shell relative to the core lies along the O-*B* bond or perpendicular to it, respectively. In the first case an additional fourth-order coupling $k_{OB,B}$ is included, which is the only anharmonic force constant of the model. Interionic short-range interactions are represented by axially symmetric harmonic force constants between the oxygen shell and those of its nearest *A*, *B*, and O ions. Finally, harmonic Coulomb interactions couple cores and shells of every ion.

The parameters of the model have the same values for $KTaO_3$ and $KNbO_3$, except for the oxygen core-shell coupling constants k_{OB} and $k_{OB,B}$. They were first determined for $KTaO_3$ by fitting the experimental phonon frequencies through a calculation within the self-consistent phonon approximation (SPA).[17] One set of parameters, including the anharmonic $k_{OB,B}$, was sufficient to reproduce the experimental data from 0 to 1200 K. Analogous calculations have been performed for $KTa_{1-x}Nb_xO_3$ with $0 \leqslant x \leqslant 1$, where it was found that only the change of k_{OB} and $k_{OB,B}$ allowed the authors to reproduce the phonon data on $KNbO_3$ at 730 K, and the temperature dependence of the ferroelectric soft mode in the paraelectric phase measured for the entire range of *x*.[29]

The model potential is

$$V(\mathbf{u},\mathbf{w}) = \frac{1}{2}\,\mathbf{u}^{\dagger}(\mathcal{S}+\mathcal{C}^{ZZ})\mathbf{u} + \frac{1}{2}\,\mathbf{w}^{\dagger}(\mathcal{S}+\mathcal{K}+\mathcal{C}^{YY})\mathbf{w} + \mathbf{u}^{\dagger}(\mathcal{S}+\mathcal{C}^{ZY})\mathbf{w} + \frac{1}{4!}\,k_{OB,B}\sum_{l\alpha} w_{\alpha}^{4}(lO_{\alpha}), \quad (1)$$

where **u** and **w** denote core and shell relative to core displacements, respectively. The short-range shell-shell interactions are represented by the matrix $\mathcal{S}$, and the Coulomb shell-shell, shell-ion, and ion-ion interactions are represented by the matrices $\mathcal{C}^{YY}$, $\mathcal{C}^{ZY}$, and $\mathcal{C}^{ZZ}$, respectively, *Y* denoting shell and *Z* ionic charges. $\mathcal{K}$ is a diagonal matrix which contains the harmonic core-shell coupling constants. The last term represents the nonlinear core-shell interaction at the O^{-2} ions, where O_{α} denotes an oxygen whose *B* neighbor ions lie in the α direction and *l* is a cell index. The adiabatic condition requires that the electronic shell configuration be a potential minimum for an arbitrary core configuration, thus leading to

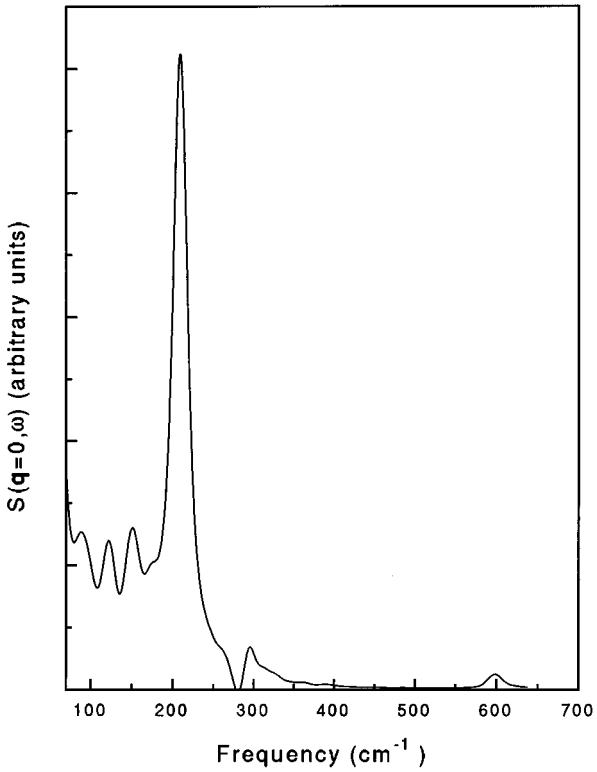

FIG. 1. Dynamical structure factor $S(\mathbf{q}=0,\omega)$ of $KNbO_3$ at 730 K, for $\mathbf{G}=(1,1,1)(2\pi/a)$, in a frequency range that includes all TO(Γ) modes.

$$\frac{\partial V}{\partial \mathbf{w}}=(\mathcal{S}+\mathcal{C}^{YZ})\mathbf{u}+(\mathcal{S}+\mathcal{K}+\mathcal{C}^{YY})\mathbf{w}+\frac{1}{3!}\,k_{\mathrm{O},B,B}\mathbf{f}(\mathbf{w})=0, \tag{2}$$

where the vector $\mathbf{f}(\mathbf{w})$ has components $f_\alpha(l\kappa)=w^3_\alpha(l\mathrm{O}_\alpha)\delta_{\kappa,\mathrm{O}_\alpha}$. With $\mathbf{w}$ implicitly determined by Eq. (2) as a nonlinear function of $\mathbf{u}$, Eq. (1) gives an effective long-range anharmonic potential for the cores.

The lattice (cores) equations of motion which correspond to the potential in Eq. (1) are

$$\mathcal{M}\ddot{\mathbf{u}}=(\mathcal{S}+\mathcal{C}^{ZZ})\mathbf{u}+(\mathcal{S}+\mathcal{C}^{ZY})\mathbf{w}, \tag{3}$$

where $\mathbf{w}$ is a nonlinear function of $\mathbf{u}$, as already explained.

The molecular-dynamics simulation reported here was carried out in the (N,V,T) ensemble, considering a supercell of $4\times4\times4$ unit cells with periodic boundary conditions. The actual cubic lattice parameter a is significant only for the dimensions of several magnitudes, since all interatomic forces are harmonic. The Coulomb matrices are calculated once (by the usual Ewald's method) as well as the short-range matrix $\mathcal{S}$, which reduces greatly the computational effort. The shell configuration $\mathbf{w}$ at each time step is obtained from Eq. (2) by iterating the following expression:

$$\mathbf{w}=-\mathcal{K}^{-1}\left[(\mathcal{S}+\mathcal{C}^{YY})\mathbf{w}+(\mathcal{S}+\mathcal{C}^{YZ})\mathbf{u}+\frac{1}{3!}\,k_{OB,B}\mathbf{f}(\mathbf{w})\right]. \tag{4}$$

The convergence is accelerated by a steepest-descent procedure. For the integration of the dynamic equations we use the following Beeman algorithm:[33]

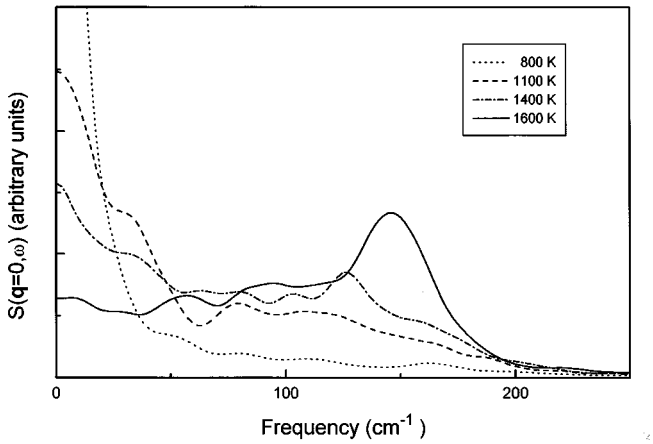

FIG. 2. Dynamical structure factor $S(\mathbf{q}=0,\omega)$ of $KNbO_3$ at several temperatures in the paraelectric phase, for $\mathbf{G}=(2,0,0)(2\pi/a)$, in the low-frequency range corresponding to the ferroelectric mode.

$$\mathbf{r}(t+\delta t)=\mathbf{r}(t)+\delta t\mathbf{v}(t)+\frac{1}{6}\,(\delta t)^2[4\mathbf{a}(t)-\mathbf{a}(t-\delta t)], \tag{5}$$

$$\mathbf{v}(t+\delta t)=\mathbf{v}(t)+\frac{1}{6}\,\delta t[2\mathbf{a}(t+\delta t)+5\mathbf{a}(t)-\mathbf{a}(t-\delta t). \tag{6}$$

For the time step we choose the value 5×10^{-15} s, which is ~10 times smaller than the smallest normal mode period.[29] We let the system evolve over 3000 time steps, which we verified are sufficient to thermalize and reach stability, and then we consider 12 000 additional time steps for the evaluation of the physical quantities.

The temperature of the system is adjusted by letting a Nosé-Hoover (NH) thermostat[34] act on each core coordinate. This is achieved by modifying the previous equations of motion (3) as follows:

$$m_i\ddot{u}_i=F_i-\eta_i m_i\dot{u}_i, \tag{7}$$

where F_i represents the right-hand side of Eq. (3), and the ''friction'' coefficient η_i of the thermostat evolves according to

$$\dot{\eta}_i=(m_i\dot{u}_i^2-k_BT)/(k_BT\tau^2). \tag{8}$$

This procedure was necessary to drive the system into thermal equilibrium. Since the anharmonic term of the NOP model couples a limited number of modes to each other (including the ferroelectric mode), many modes do not interchange energy. As a consequence, the temperature of the coupled modes may differ from the mean temperature of the system, depending on the initial conditions of the simulation. This led us to a wrong evaluation of temperature and possibly also to distortions of the dynamical structure factor in our preliminary calculations,[32] where the temperature was fixed by rescaling particle velocities after each step. The usual NH procedure of applying a unique thermostat (single η) to every degree of freedom also did not help to achieve thermal equilibrium.

The dynamical structure factor $S(\mathbf{q},\omega)$ is evaluated as the space-time Fourier transform of the core-core displacement correlation function:

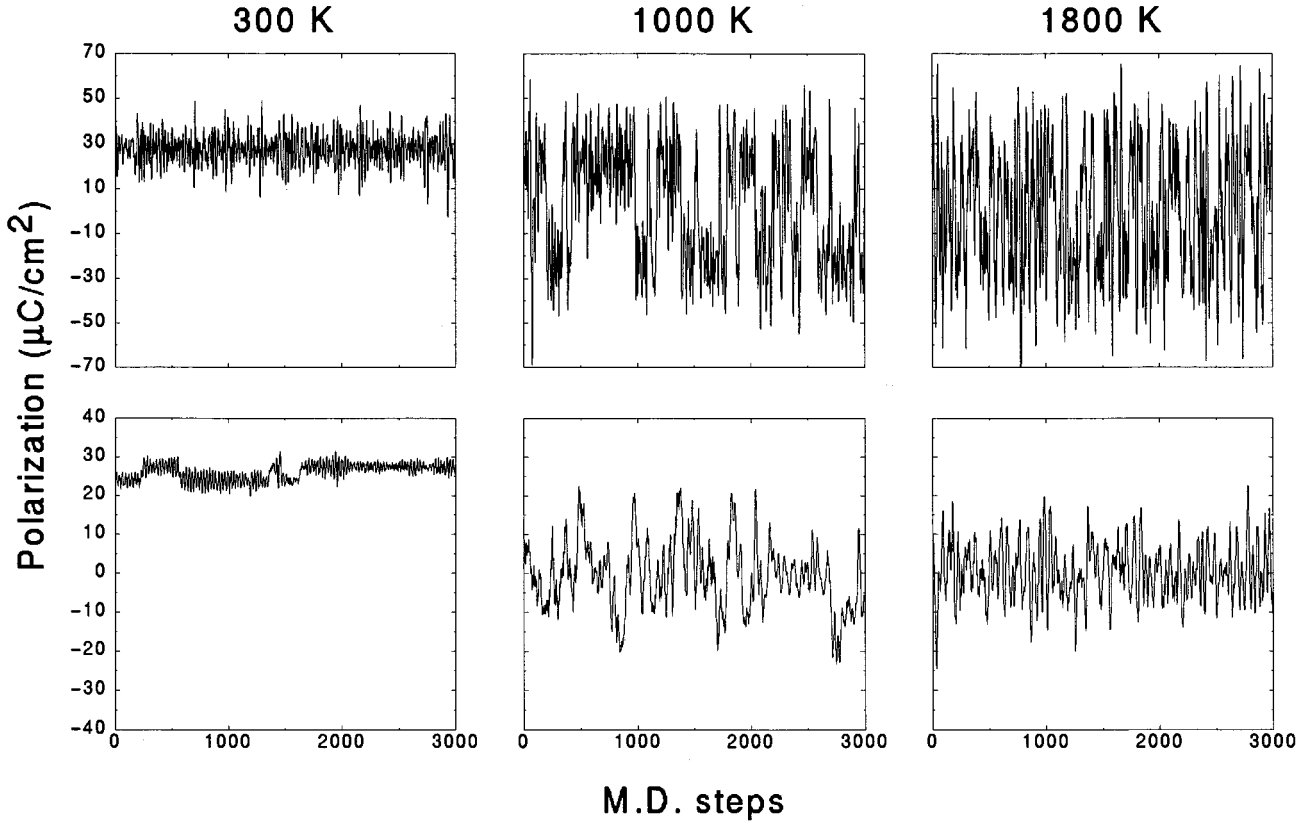

FIG. 3. Time evolution of the polarization in a single cell (above) and in the supercell (below) at several temperatures in $KNbO_3$.

$$S(\mathbf{Q},\omega)=\int_{-\infty}^{+\infty} dt\, e^{i\omega t}\sum_{l\kappa}\sum_{l'\kappa'} e^{i\mathbf{Q}\cdot(\mathbf{R}_\kappa^l-\mathbf{R}_{\kappa'}^{l'})} \times\langle \mathbf{Q}\cdot\mathbf{u}_\kappa^l(t)\mathbf{Q}\cdot\mathbf{u}_{\kappa'}^{l'}(0)\rangle, \quad (9)$$

where $\mathbf{Q}$ is an arbitrary wave vector, which can be decomposed in a reciprocal-lattice vector $\mathbf{G}$ and a wave vector $\mathbf{q}$ within the first Brillouin zone, $\mathbf{Q}=\mathbf{G}+\mathbf{q}$. To analyze the zone-center modes we calculate $S(\mathbf{0},\omega)$ by the so-called *direct approach.*[35] The choice of $\mathbf{G}$ affects the relative intensities of peaks corresponding to different modes. A Gaussian smoothing procedure is applied to the correlation function before the time Fourier transform is performed.

III. RESULTS AND DISCUSSION

A. $KNbO_3$

We show in Fig. 1 the dynamical structure factor $S(\mathbf{0},\omega)$ for $KNbO_3$ at $T=730$ K in a frequency range that extends up to the highest TO modes. The LO modes do not appear to be split from the TO ones because we do not include the macroscopic field. Thus each peak in Fig. 1 corresponds to a triple degenerate optical mode. We select the reciprocal-lattice vector $\mathbf{G}=(1,1,1)(2\pi/a)$ in Eq. (9), such as to obtain enough intensity for the high-frequency modes. By comparison with the SPA results[29] we identify the peak at 300 cm^{-1} as due to the silent mode of Γ_{25} symmetry, and the peaks at 210 and 600 cm^{-1} correspond to higher infrared-active modes of Γ_{15} symmetry. No evidence shows up of the lowest Γ_{15} mode, i.e., the ferroelectric one, which should appear below 200 cm^{-1}. We cannot assign the structures observed in this frequency range to anything else than effects of the numerical integration.

We search for evidence of the ferroelectric mode at increasingly higher temperatures and try with several $\mathbf{G}$ vectors. As shown in Fig. 2 for $\mathbf{G}=(2,0,0)(2\pi/a)$ no well-defined structure appears below the melting point of the material (1323 K). On the other hand, we observe a quasi-elastic component of $S(\mathbf{0},\omega)$ (central peak) which sharpens and grows in intensity with decreasing temperature. As we will further discuss below, this is the signature of a relaxational dynamics characteristic of an order-disorder transition mechanism. Nevertheless, with the aim to observe if a crossover to a soft-mode dynamics can be detected in $S(\mathbf{0},\omega)$, we increase the temperature of our simulations above the actual melting point. A wide structure in the 70–140 cm^{-1} frequency interval at 1100 K develops a peak at $\sim$125 cm^{-1} as the temperature is increased to 1400 K. This peak, which corresponds to the ferroelectric mode, shifts to higher frequency and gains intensity as the temperature is further increased to 1600 K. This dynamical behavior constitutes theoretical evidence for the existence of a crossover from a displacive to an order-disorder regime to explain the mechanism of the ferroelectric phase transition in $KNbO_3$.

We distinguish two dynamic regimes as a function of temperature, one signed by the presence of the soft mode above $\sim$1400 K, and another signed by the central peak below $\sim$1100 K. To characterize the particle dynamics in these two regimes we plot in Fig. 3 the time evolution of the polarization in a single unit cell and that of the whole supercell

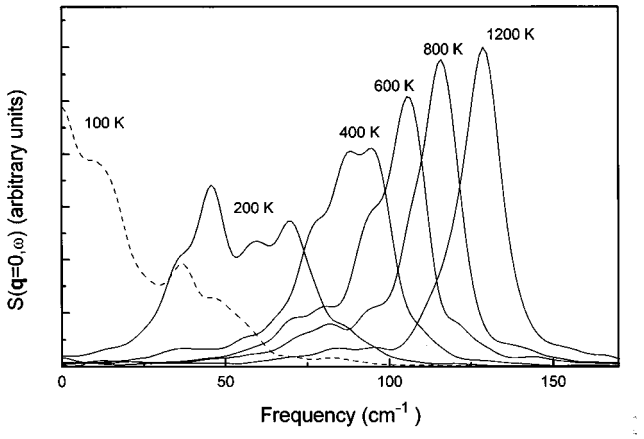

FIG. 4. Dynamical structure factor $S(\mathbf{q}=0,\omega)$ of $KTaO_3$ at several temperatures.

at different temperatures. To make evident the behavior described below we take 3000 of the total 12 000 time steps. At 1800 K (high-temperature regime) only fast oscillations around zero polarization are observed for both the single cell and the supercell. At 1000 K (low-temperature regime), the coexistence of fast oscillations around finite polarization values with slower changes in the polarization sign is clearly seen for the case of a single cell. The critical motion, therefore, possesses two components with different time scales. While one component is associated with oscillations about quasiequilibrium positions and give the phonon feature, the other corresponds to a relaxational motion between equiprobable positions. From the mean frequency of the polarization sign changes at 1000 K, we can roughly estimate the inverse relaxation time as $\sim 27\ \mathrm{cm}^{-1}$, which is in quite good agreement with the value fitted from the experiments.[8] We verified that the polarization reversals become less frequent upon cooling, which is related to the narrowing of the central component of $S(\mathbf{0},\omega)$.

The supercell polarization at a given temperature shows a less regular time evolution than a single cell (see, e.g., the plots for 1000 K in Fig. 2). This behavior should be related with a restricted correlation between polarizations of different unit cells. The central peak intensity growth with decreasing temperature should reflect an increase of this correlation. In fact we observe also in the supercell a slowing down of the polarization reversals while cooling. Nevertheless, at least one reversal appeared in the observation interval of 12 000 time steps up to temperatures as low as 350 K. At 300 K no reversal was observed, and the system may be considered to be in the ferroelectric phase. At this temperature the three polarization components turned out to be equal, which corresponds to the rhombohedral phase. We recall that it has been predicted in the framework of the eight-site model, that only the direct transition to the lowest energy phase will occur if the cubic lattice is rigid maintained, thus not allowing for the homogeneous deformations present in the various phases.[6] We obtain at 300 K a polarization of $\sim 45\ \mu\mathrm{C/cm}^2$.

B. $KTaO_3$

In Fig. 4 we show the dynamical structure factor for $KTaO_3$ at $\mathbf{q}=0$ at several temperatures between 0 and 1200 K. As in $KNbO_3$ we take $\mathbf{G}=(2,0,0)(2\pi/a)$ for a better display of the ferroelectic mode peak. This is quite well defined and softens steadily over the whole temperature range. As shown in Fig. 5, the frequencies at which the peaks are centered have a temperature dependence in good agreement compared with inelastic neutron-scattering data in the same temperature range, and also with results of the SPA calculations.[17]

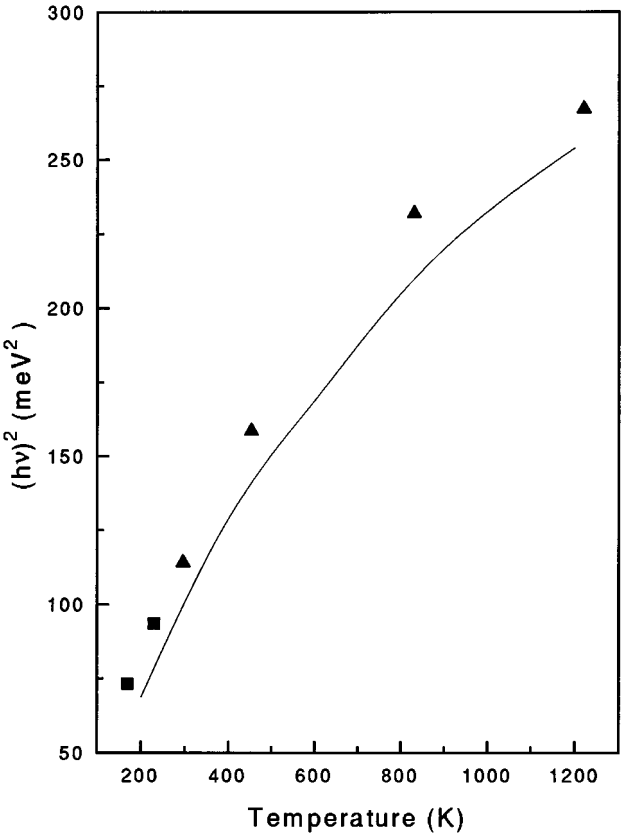

FIG. 5. Temperature dependence of the ferroelectric soft-mode peak in $KTaO_3$ (full line) compared to the experimental neutron data (Ref. 17) (square dots).

The energy as a function of Ta displacements evaluated with the NOP model shows a very flat minimum at the centrosymmetric position,[1] which agrees with an *ab initio* result.[3] However, if the other ions are also allowed to displace according to the ferroelectric mode eigenvector, off-centered minimums only 0.05 mRy below the centrosymmetric maximum appear.[1] Therefore a quasiharmonic dynamics is expected for the ferroelectric mode in this effective potential. This is reflected in the sharpness of the high-temperature peaks in Fig. 4, and in the fact that the SPA works well for this material. In contrast with the good agreement obtained for the ferroelectric mode frequency, its width increases with decreasing temperature, which contradicts the experimental observation.[16] This result of the simulation seems plausible for the classical dynamics of a system which exhibits an effective double-well potential. In fact, one expects the soft mode to be increasingly coupled to the relaxation mode as the temperature decreases, thus leading to a higher damping. On the other hand, anharmonic perturbation theory would lead to a decrease of the damping with temperature due to a

smaller decay of the soft mode into other phonons. Such a theory could be applied only if there is no instability at the cubic centrosymmetric phase. Therefore, we can speculate on the possibility that the effective potential for the soft mode is actually very flat but with no off-center minima. This is a point which has been recently discussed.[3,36] In addition, the very large peak width observed at 200 K, and the central peak which appears below this temperature (Fig. 4) can be considered a spurious effect of the classical simulation, where zero-point quantum fluctuations are not considered. These fluctuations provide energy to the soft mode.

IV. CONCLUSIONS

The dynamics of the NOP model confirms a crossover from a displacive to an order-disorder mechanism for the paraelectric-ferroelectric transition in $KNbO_3$, as has been proposed to interpret various experiments. The order-disorder behavior extends in the paraelectric phase over several hundred degrees above the experimental transition temperature to the tetragonal phase and explains the relaxation phenomena observed in the experiments. The soft mode, which has not been directly observed but postulated as an overdamped oscillator to adjust the experimental data, appears as a distinct peak of $S(\mathbf{q}=0,\omega)$ at temperatures above the range of available experimental data.

Due to the constant-volume treatment performed, the simulation leads to a direct transition to the lowest ferroelectric phase, with [111] polarization. To obtain the intermediate tetragonal and orthorhombic phases it is necessary to perform a constant-pressure simulation considering interionic potentials instead of force constants. This study, which is in progress, could also help to elucidate the nature of dynamical correlations near the cubic-tetragonal phase transition in $KNbO_3$. The dynamical structure factor of $KTaO_3$ shows the ferroelectric mode as a sharp peak which shifts with temperature in quite good agreement with experiments and with results from the SPA for the model.

ACKNOWLEDGMENTS

We thank J. Kohanoff for advice on the molecular-dynamics technique. We acknowledge support from Consejo Nacional de Investigaciones Científicas y Técnicas de la República Argentina and from Consejo de Investigaciones de la Universidad Nacional de Rosario.

[1] M. Sepliarsky, M. G. Stachiotti, and R. Migoni, Phys. Rev. B **52**, 4044 (1995).
[2] P. Edwarson, Phys. Rev. Lett. **63**, 55 (1989).
[3] A. Postnikov, T. Neumann, G. Borstel, and M. Methfessel, Phys. Rev. B **48**, 5910 (1993).
[4] N. de Mathan, E. Prouzet, E. Husson, and H. Dexpert, J. Phys. Condens. Matter **5**, 1261 (1993).
[5] R. Comes, R. Lambert, and A. Guinier, Solid State Commun. **6**, 715 (1968); Acta Crystallogr. A **26**, 244 (1970).
[6] S. Chaves, F. C. S. Barreto, R. A. Nogueira, and B. Zeks, Phys. Rev. B **13**, 207 (1976).
[7] M. D. Fontana, G. Métrat, J. Servoin, and F. Gervais, J. Phys. C **16**, 483 (1984).
[8] M. D. Fontana, A. Ridah, G. E. Kugel, and C. Carabatos-Nedelec, J. Phys. C **21**, 5853 (1988).
[9] J. P. Sokoloff, L. L. Chase, and D. Rytz, Phys. Rev. B **38**, 597 (1988).
[10] K. A. Müller, Y. Luspin, J. L. Servoin, and F. Gervais, J. Phys. (France) Lett. **43**, L-537 (1982).
[11] K. A. Müller and W. Berlinger, Phys. Rev. B **34**, 6130 (1986).
[12] M. Maglione, R. Böhmer, A. Loidl, and U. Höchli, Phys. Rev. B **40**, 11 441 (1989).
[13] C. H. Perry and T. F. McNelly, Phys. Rev. **154**, 456 (1967).
[14] G. Shirane, R. Nathans, and V. J. Minkiewicz, Phys. Rev. **157**, 396 (1967).
[15] P. Fleury and J. Worlock, Phys. Rev. **164**, 613 (1968).
[16] H. Vogt and H. Uwe, Phys. Rev. B **29**, 1030 (1984).
[17] C. Perry, R. Currat, H. Buhay, R. Migoni, W. Stirling, and J. Axe, Phys. Rev. B **39**, 8666 (1989).
[18] M. Maglione, S. Rod, and U. T. Höchli, Europhys. Lett. **4**, 631 (1987).
[19] H. Vogt, M. D. Fontana, G. E. Kugel, and P. Günter, Phys. Rev. B **34**, 410 (1986).
[20] Y. Luspin, J. L. Servoin, and F. Gervais, J. Phys. C **13**, 3761 (1980).
[21] H. Vogt, J. Sanjurjo, and G. Rossbroich, Phys. Rev. B **26**, 5904 (1982).
[22] T. Schneider and E. Stoll, Phys. Rev. B **13**, 1216 (1975); **17**, 1302 (1978).
[23] J. A. Krumhansl and J. R. Schrieffer, Phys. Rev. B **11**, 3535 (1975).
[24] A. D. Bruce, Adv. Phys. **29**, 111 (1980).
[25] R. Migoni, H. Bilz, and D. Bäuerle, Phys. Rev. Lett. **37**, 1155 (1976).
[26] R. Cohen and H. Krakauer, Phys. Rev. B **42**, 6416 (1990).
[27] R. D. King-Smith and D. Vanderbilt, Phys. Rev. B **49**, 5828 (1994).
[28] M. Posternak, R. Resta, and A. Baldereschi, Phys. Rev. B **50**, 8911 (1994).
[29] G. E. Kugel, M. D. Fontana, and W. Kress, Phys. Rev. B **35**, 813 (1987).
[30] D. Khatib, R. L. Migoni, G. E. Kugel, and L. Godefroy, J. Phys. Condens. Matter **1**, 9811 (1991).
[31] M. Stachiotti, A. Dobry, R. Migoni, and A. Bussmann-Holder, Phys. Rev. B **47**, 2473 (1993).
[32] M. Sepliarsky, R. Migoni, and M. G. Stachiotti, Ferroelectrics **183**, 105 (1996).
[33] D. Beeman, J. Comput. Phys. **20**, 130 (1976).
[34] W. G. Hoover, Phys. Rev. A **31**, 1695 (1985).
[35] M. P. Allen and D. J. Tildesley, *Computer Simulation of Liquids* (Clarendon, Oxford, 1987), p. 185.
[36] D. J. Singh, Phys. Rev. B **53**, 176 (1996).